*Science of Sintering*, **55** (2023) 437-452

https://doi.org/10.2298/SOS230414042A

UDK: 691.73; 539.375; 692.533.1

# An Examination of Microstructure, Microhardness and Tribological Properties of Ceramic Reinforced Bronze Matrix Composite Materials

**Hakan Ada[1,2*)], Emine Türkmen[3], Yavuz Kaplan[4], Elif Özçatalbaş[3], Ender Yetkin Şatir[2], Sinan Aksöz[5]**

[1]Gazi University, Faculty of Technology, Department of Metallurgical and Materials Engineering, Ankara, 06500, Türkiye
[2]Kastamonu University, Faculty of Engineering and Architecture, Department of Mechanical Engineering, Kastamonu, 37150, Türkiye
[3]Kastamonu University, Institue of Science, Department of Mechanical Engineering, Kastamonu, 37150, Türkiye
[4]Pamukkale University, Faculty of Technology, Department of Mechanical and Manufacturing Engineering, Denizli, 20160, Türkiye
[5]Pamukkale University, Faculty of Technology, Department of Metallurgical and Materials Engineering, Denizli, 20160, Türkiye

***Abstract:***

*In order to obtain better mechanical properties in a bronze alloy, it is important to produce new materials by adding reinforcements and to offer these materials to the industry. In this study, bronze matrix (Cu10Sn) materials were reinforced with boron carbide ($B_4C$) and silicon carbide (SiC) ceramic materials by using the mechanical alloying method. New composite materials were produced by powder metallurgy method by adding ceramic reinforcement ($B_4C$ and SiC) at 1, 2, 4 and 8 weight ratios to Cu10Sn alloy, which is the main matrix material. The obtained composite materials examined in terms of structural, microhardness and wear resistance. Coefficient friction, specific wear rate and volume loss rates under 5N, 10N, and 15N loads were examined for the samples produced. When the applied microhardness and wear behaviors were examined, it was generally seen that the hardness and wear behaviors were improved with the added reinforcement ratios. In line with the examinations made, based on the hardness and wear processes applied to the materials consisting of the bronze matrix of the reinforcement material, it was observed that the most appropriate results were obtained from composite materials (Alloy 4 and Alloy 8), which contain 4% $B_4C$ and SiC reinforcement.*

***Keywords***: *Powder metallurgy; Bronze; Composite; Wear; Microhardness.*

## 1. Introduction

Low-density (light), rigid, and high-strength materials are needed in many engineering applications used in the industry [1]. In line with all these needs, it is necessary to use materials with excellent properties to produce products with superior functionality. Composite materials are materials formed by combining two or more components that are

*) **Corresponding author:** drhakanada@gmail.com

practically insoluble in each other, in order to produce innovative materials with new and desired qualities to obtain superior properties from different components. Composite materials are generally formed by dispersing a low-strength, low-elastic modulus matrix and a smaller amount of reinforcing element in the structure compared to the matrix [2]. With the composite materials produced, it is aimed to develop new materials with the required properties [3]. The properties of composite materials have become adjustable through a selection of matrices and reinforcements. In composite materials where the reinforcement phase has micrometer-sized grains, small additions to the reinforcement material can significantly affect mechanical properties [4]. Metal matrix composites (MMC) are a product consisting of one or more reinforcing materials with the main matrix [5-7]. The properties of this material greatly depend on the shape, size, and volume of the supplement added [8-11]. MMC materials have been used extensively in the aerospace, automotive, and defense industries, although they have had an important place in many research and application fields from the past to the present [2, 12, 13].

Copper and its alloys are widely used for automotive applications due to their good thermal conductivity, excellent fatigue strength and high wear resistance, which can have potential for many applications such as bearings, brakes, clutches and sleeves [14]. For large-scale electrical equipment, it is difficult to achieve current transfer from one material to another through contact on the surface. While such contact requires extreme contact pressure, it is important to minimize friction and wear on the material. Cu alloys are used in various applications because they have very good thermal-electrical conductivity and favorable corrosion resistance [15, 16]. One of the copper alloys widely used in the industry is bronze (Copper-Tin) alloys, which are mostly preferred as bearing materials and generally have 90% Cu and 10% Sn content (Cu10Sn) [17]. Bronze alloys have high wear resistance and the wear resistance of the material increases further depending on the amount of Tin added [18]. Bronze used as a bearing material is a suitable alloy for use in large and impact loads, as well as at high temperatures where there is a risk of corrosion [19]. Among MCCs, copper matrix composites have become popular in recent years. Pure copper cannot be used in stand-alone applications due to its low strength and not very good physical properties [20, 21]. Copper matrix composite materials are used in electrical contacts, electrodes, electronic materials, cutting tools and structural applications requiring high performance [22]. By adding one or more reinforcing materials to pure copper, the mechanical and physical properties can be significantly improved, even at high temperatures, without major changes in the thermal and conductive properties of the base matrix [23-25]. Many researchers have found controllable properties such as high thermal conductivity, good fatigue strength, low thermal expansion coefficient and high wear resistance when reinforcement particles are added to the Cu alloy matrix [15, 26, 27]. Materials with Cu matrix are reinforced with particles such as silicon carbide (SiC) and boron carbide ($B_4C$) to obtain important properties such as hardness and wear resistance [15, 27-29].

Islak and Abushraida examined the microstructures and hardness properties of the samples obtained by adding boron carbide ($B_4C$), silicon carbide (SiC), titanium carbide (TiC), and molybdenum carbide ($Mo_2C$) to the Cu10Sn matrix in their study, where they applied the powder metallurgy method. In the study, the highest hardness was measured in the Cu10Sn-$B_4C$ composite with a value of 212 $HV_{0.2}$. As a result of this study, it was suggested that wear and corrosion behaviors could be examined by conducting wear and corrosion tests on the samples [30]. İpek et al. added 2, 4, 6, 8 and 10% $B_4C$ to the Cu matrix and stated that the hardness values increased due to the increased reinforcement rate. In addition, it has been observed in the study that wear loss decreases with an increase in sintering time [31]. Veerappan et al. reinforced three different proportions (2%, 4%, 6%) of Ni into the bronze matrix, and found that the composite material containing 4% Ni by weight exhibited the highest compressive strength, and the composite material containing 6% Ni exhibited the highest hardness and corrosion resistance [32]. Bunlangsup et al. determined that composite materials obtained by adding a natural anhydride ($CaSO_4$) powder to the Cu-8Sn bronze matrix by the T/M method had a slight increase in hardness with the increase in anhydride content due to the porous microstructure of the multiphase material [33]. Shunmugam et al. T/M produced bronze electrodes and determined that the electrode could be used in tribological applications involving excessive pressure and speed [34]. Abhik et al., on the other hand, determined that the wear resistance of composite materials decreases when the reinforcement element ratio exceeds a certain limit [35].

While the rarity of studies using $B_4C$ and SiC as reinforcing elements with bronze matrix (Cu10Sn etc.) is interesting to note in the literature studies obtained, no studies on the wear behavior of $B_4C$ and SiC reinforced Cu10Sn matrix composite materials have been encountered. In this study, bronze matrix and different types of ceramic (SiC, $B_4C$) reinforced composite materials, which are found to be lacking in the literature, were used, and their wear behavior was examined in detail. The rates required for the reinforcement materials in the study were determined based on the rates specified in similar studies [36, 37]. In the study, primarily the effects of the reinforcement element on the microhardness and wear performance of the matrix structure were revealed by conducting microhardness and wear tests after the characterization of the produced composite materials in terms of microstructure.

## 2. Materials and Experimental Procedures

The powders used in this study were obtained from Nanokar company. Cu10Sn powders consisting of 90% Cu and 10% Sn with a size of 44 µm and 85% purity were used as the main matrix material, and SiC with a size of <45µm and 99.5% purity and $B_4C$ powders with a size of <45 µm and 99.5% purity were used for reinforcement materials are given in Fig. 1. In the first stage of the production of composite materials, the powder ratios were determined. In the determination of the ratios, the most appropriate weight ratios according to the literature were taken as a basis. High-purity powders were mixed at 200 rpm speed for 60 minutes and with a 10/1 ball/powder ratio in a Retsch brand PM100 model device in the Mechanical Engineering Laboratories of Kastamonu University, Faculty of Engineering and Architecture, in percentage by weight shown in Table I and subjected to the mechanical alloying process.

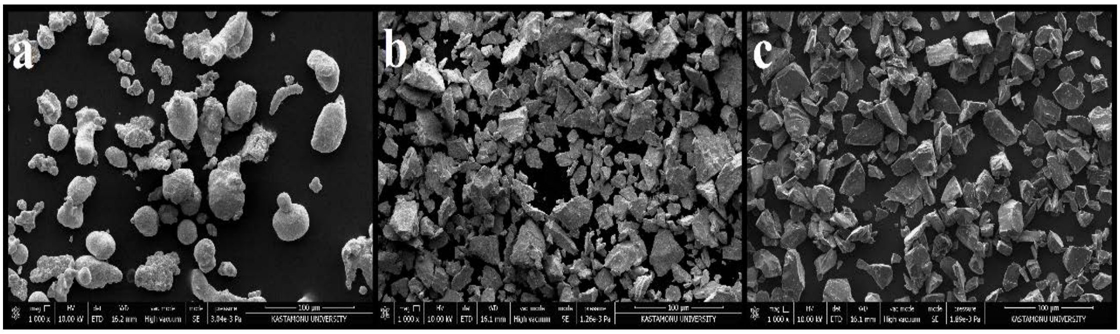


**Fig. 1.** Powders used in the study. a) Cu10Sn, b) $B_4C$, c) SiC.

Bronze matrix and ceramic reinforced mixture powders subjected to mechanical alloying at the rates specified in Table I were then subjected to cold pressing processes in a unidirectional axial press under 500 MPa pressure. After the cold pressing process, the samples were sintered at 750 ºC for 90 minutes, and the production of composite material was completed. The diagram explaining the production process of the materials is given in Fig. 2, and the photos of the produced materials are given in Fig. 3.

**Tab. I** Composite materials produced and mixing ratios (% by weight).

| Alloy Number | Cu10Sn (%) | $B_4C$ (%) | SiC (%) |
|---|---|---|---|
| **1** | 100 | - | - |
| **2** | 99 | 1 | |
| **3** | 98 | 2 | |
| **4** | 96 | 4 | |
| **5** | 92 | 8 | |
| **6** | 99 | | 1 |
| **7** | 98 | | 2 |
| **8** | 96 | | 4 |
| **9** | 92 | | 8 |

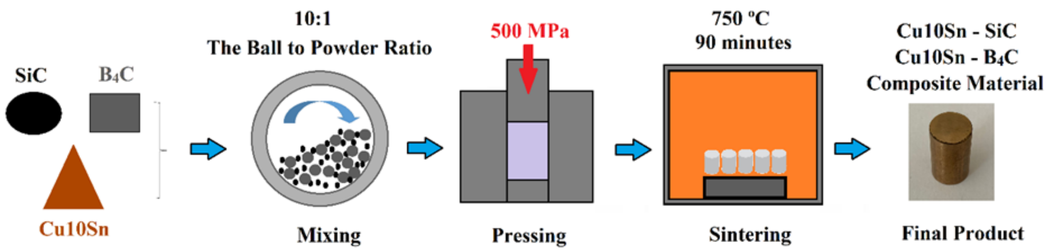


**Fig. 2.** The manufacturing process of composite materials.

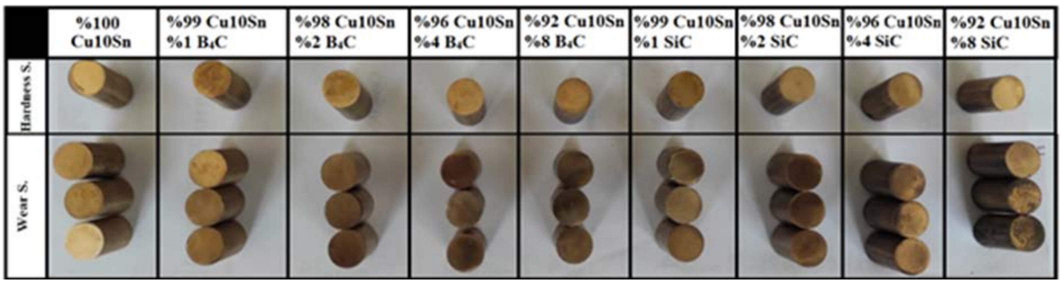


**Fig. 3.** Manufactured composite materials.

Microstructure, microhardness, and wear properties of Cu10Sn-$B_4C$ and Cu10Sn-SiC (the produced composite materials) were investigated. Optical microscope examinations of the samples were carried out with a Nikon brand, MA100 model optical microscope, SEM and EDS examinations were carried out with a FEI Quanta FEG 250 brand and model device, and the microhardness examinations were carried out using a Shimadzu HVM-2 brand and model device with the Vickers hardness measurement method using a 136° pyramidal diamond indenter. In microhardness measurements, a total of 25 measurements were made from 5 different regions of the sample at 5 different loads (0.245 N, 0.490 N, 0.980 N, 1.960 N, 2.940 N) and the average microhardness values were calculated. In addition, the samples were subjected to an wear test to determine the wear resistance of composite materials. All wear tests were carried out according to ASTM standard G99 using a pin-on-disk apparatus under dry test conditions. Wear tests were carried out at a distance of 1000 m, at a speed of 1 m/s, under 5 N, 10 N and 15 N loads. The Ø10 × 15 mm Cu10Sn matrix specimens were used with an abrasive disk (Ø60 × 12 mm) of AISI 52100 steel. The hardness value of the disk material was determined as 60 HRC. Microstructure examinations and microhardness tests of the samples were carried out at Kastamonu University, Faculty of Engineering and Architecture

Laboratories; and the wear tests were carried out at Pamukkale University, Faculty of Technology Laboratories.

## 3. Results and Discussion
### 3.1. Microstructure Reviews

Microstructure and SEM images of composite materials consisting of main matrix material Cu10Sn and SiC and $B_4C$ in different proportions are given in Fig. 4 and Fig. 5, respectively.

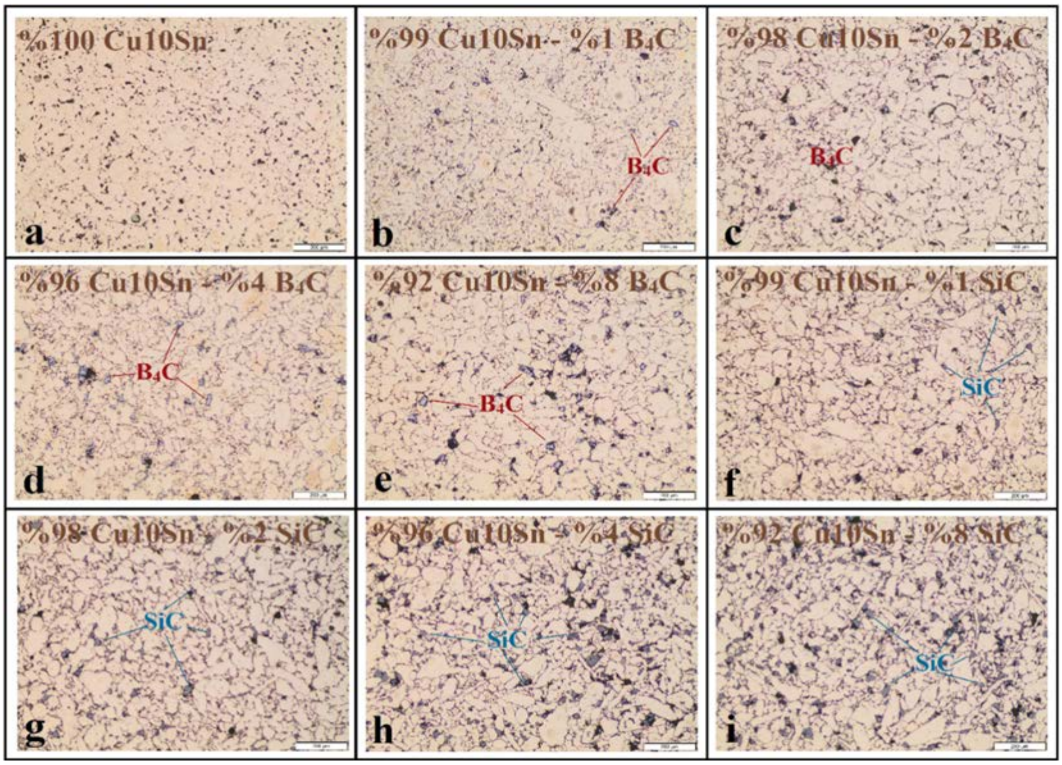


**Fig. 4.** Microstructure images taken from the samples: a) %100 Cu10Sn, b) %99 Cu10Sn - %1 $B_4C$, c) %98 Cu10Sn - %2 $B_4C$, d) %96 Cu10Sn - %4 $B_4C$, e) %92 Cu10Sn - %8 $B_4C$, f) %99 Cu10Sn - %1 SiC, g) %98 Cu10Sn - %2 SiC, h) %96 Cu10Sn - %4 SiC, i) %92 Cu10Sn - %8 SiC).

In microstructure images, the light-colored grains are bronze alloy grains, while $B_4C$ particles are seen in gray color, and SiC particles are seen in a darker color. It is observed from the microstructure and SEM images that the bronze alloy is formed coaxially and in different sizes. $B_4C$ and SiC particles are in both coaxial and flat form and are observed to be formed in smaller sizes than bronze grains. It is also understood from the microstructure and SEM images that $B_4C$ and SiC particles show a homogeneous distribution in the bronze matrix structure. Torabi & Arghavinian, Yener and Efe mentioned in their studies that the $B_4C$ and SiC particles in the images obtained on the copper matrix have the structure and distribution similar to our study [27, 38, 39].

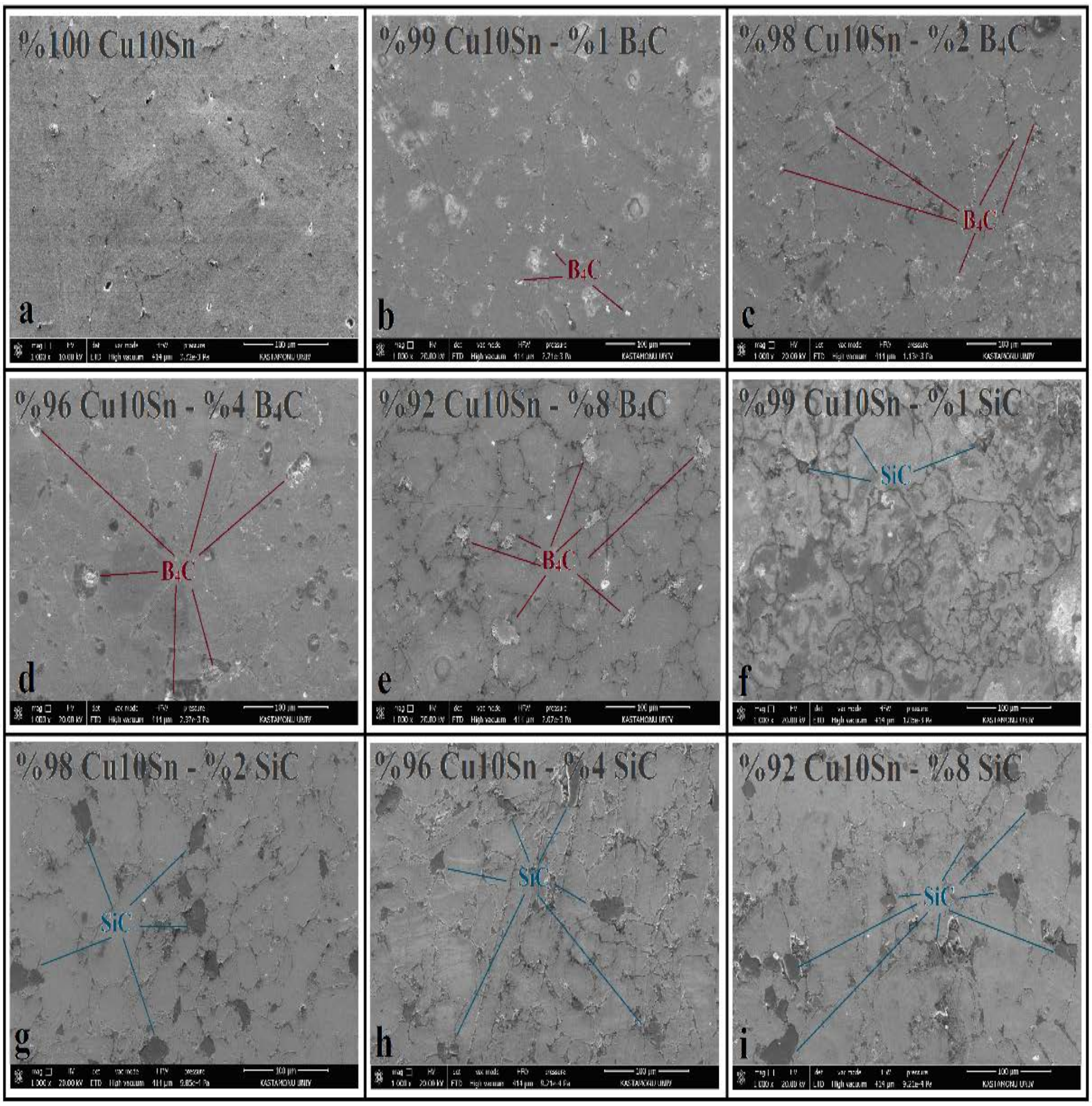


**Fig. 5.** SEM images taken from the samples: a) %100 Cu10Sn, b) %99 Cu10Sn - %1 $B_4C$, c) %98 Cu10Sn - %2 $B_4C$, d) %96 Cu10Sn - %4 $B_4C$, e) %92 Cu10Sn - %8 $B_4C$, f) %99 Cu10Sn - %1 SiC, g) %98 Cu10Sn - %2 SiC, h) %96 Cu10Sn - %4 SiC, i) %92 Cu10Sn - %8 SiC.

## 3.2. EDS Analyses

SEM images and field-screened EDS analyses, with the results given in Fig. 6, were obtained on the samples. In the EDS analyses, the results of the samples with the lowest and highest ratios of SiC and $B_4C$ doped together with the undoped sample were examined. In the EDS analyses, the elements containing the matrix - reinforcement materials and the changes in reinforcement ratios were determined.

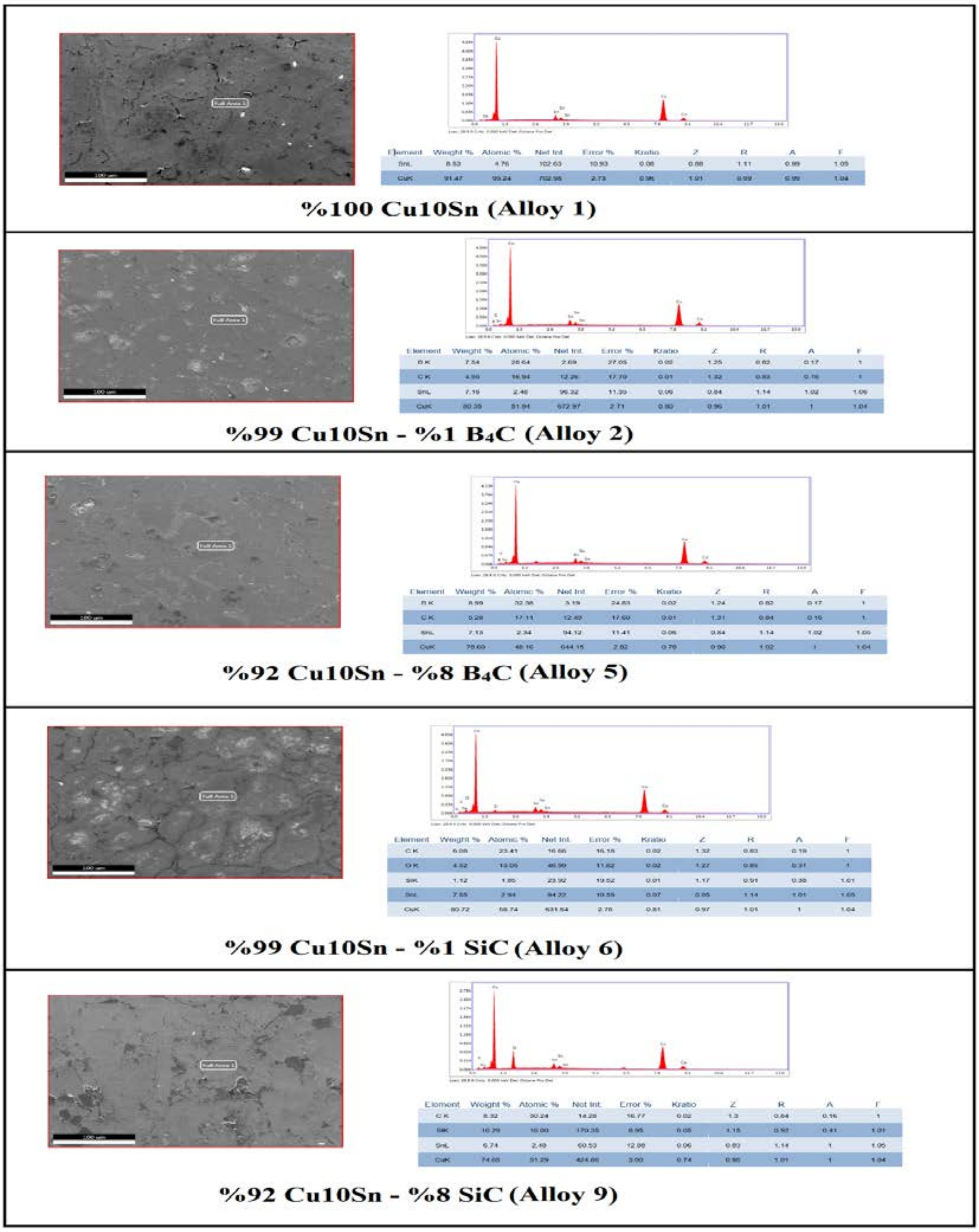


**Fig. 6.** EDS results obtained from the SEM image of composite materials.

## 3.3. Microhardness Measurements

The plots showing the hardness change in the material (in the range of 0.245 N to 2.940 N) depending on the load applied in the composite materials with the addition of the reinforcement ratio in Cu10Sn - $B_4C$ and Cu10Sn - SiC composite materials are given in Fig. 7.

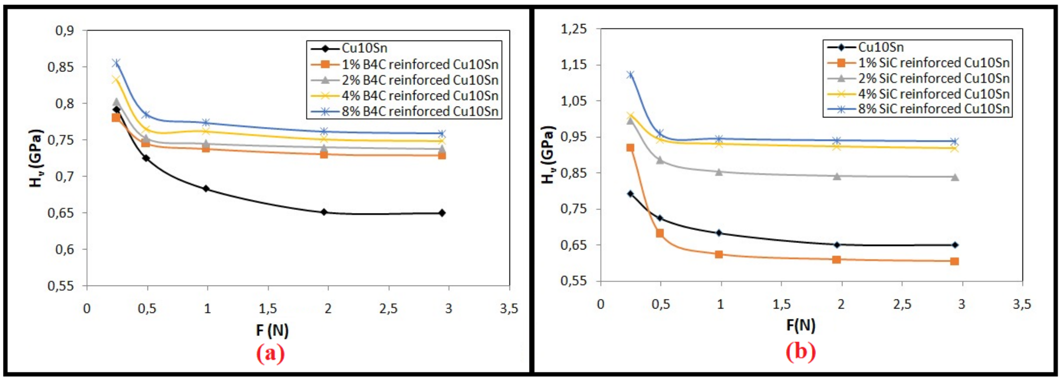


**Fig. 7.** Microhardness graph.

As can be seen from the plots, the decrease in hardness is noteworthy with the increase in the load applied during the tests. It was determined that the composite materials produced due to the decrease in hardness with the increase of the load showed Indentation Size Effect (ISE) behavior in the microhardness behavior. It is also seen that the hardness values of all samples do not change after approximately 1 N. This region, where the hardness does not change, is called the plateau region. In short, there is almost no significant change in the hardness of the material at loads greater than 1 N. This result obtained in the study shows similarities to the results obtained in other studies [40, 41].

When compared with the sample without additives, the hardness values of the material change with $B_4C$ and SiC additives. The hardness values of the samples increased with the addition of 1%, 2, 4, and 8% of $B_4C$. When only 1% SiC-doped composite material was compared with the unadulterated sample, it was observed that there was a significant decrease in hardness, except that the added composite materials in all samples reached higher hardness values than the unadulterated matrix material. From here, it is possible to say that there is a directly proportional increase between the increase in the reinforcement ratio and the hardness results. It is thought that the decrease in hardness with a 1% SiC contribution and negligible level may be related to the condition and irregularity of the impurity phases. It is also known that these factors cause the weakening of strong bonds, and consequently, a decrease in stiffness. The highest results were obtained from alloys with a reinforcement ratio of 8%. In the measurements made for the alloy using an 8% $B_4C$ reinforcement, the hardness in the plateau region formed with the increasing load was measured as approximately 0.8 GPa, while the hardness in this region was determined as 0.95 GPa in the alloy containing 8% SiC. In the results; due to the presence of carbide-based particles that increase hardness in composite materials in general, the increase in hardness with the increase in $B_4C$ and SiC reinforcement ratios has attracted attention. Similar studies on this subject also confirm the microhardness results obtained [18, 19, 25, 27, 30, 31, 38].

## 3.4. Wear experiments

Fig. 8 shows the volume loss of $B_4C$ and SiC-reinforced Cu10Sn material, and Fig.9 shows the wear rate (SWR) graphics. SWR provides detailed information about the tribological properties of the material, including all test parameters [3, 42]. Generally the volume loss and SWR values of Cu10Sn material with $B_4C$ and SiC added at different rates are lower than Cu10Sn without reinforcement at all additive ratios. The plots clearly shows that reinforcement with $B_4C$ and SiC increases the wear resistance of Cu10Sn. In the results obtained in wear studies for composite materials produced by powder metallurgy, it was found that the volume loss and SWR results with B4C and SiC reinforcement were lower than the results of the main matrix, similar to the results in our study [43-45]. Although a generally similar situation applies in the SiC-reinforced Cu10Sn, different results were obtained in the 8% SiC-reinforced test sample. The volume loss results of the 8% SiC reinforced Cu10Sn test sample are very similar to the results of Cu10Sn without reinforcement. The reason for this is thought to be that the reinforcement material breaks off from the surface during the experiment and this is reflected in the weight loss and thus in the volume loss. In addition, since all pressing operations are carried out under the same pressure, the pressure applied to 8% SiC reinforcement Cu10Sn may not be sufficient. This may have caused spills during the wear test. When the reinforcement rates were compared, it was determined that there was no significant difference between the volume loss values. With the increase in the applied load, an increase in volume loss occurred in all test parameters, as expected. While the volume loss of $B_4C$ reinforced Cu10Sn under a 5N load was approximately 0.5 $mm^3$, the volume loss of unreinforced Cu10Sn was approximately 2.6 times with a result as much as 2.3 $mm^3$. This ratio is almost similar in experiments where 10N and 15N loads are applied.

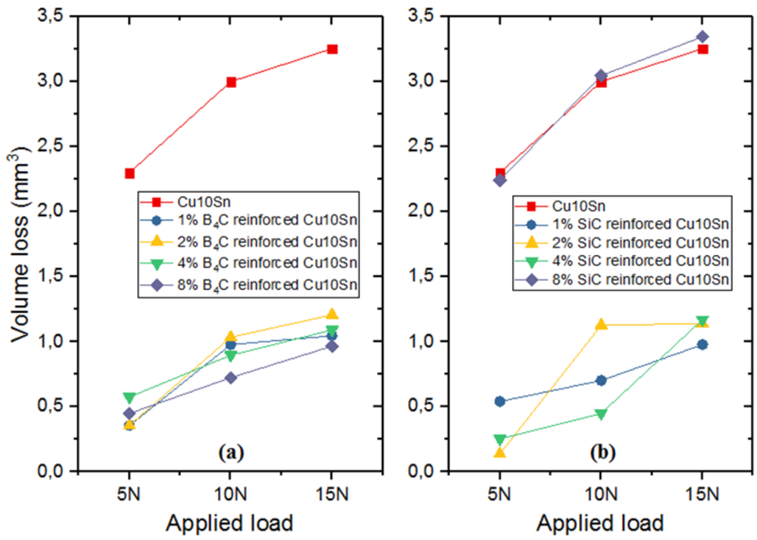


**Fig. 8.** Volume loss graph of $B_4C$ (a) and SiC (b) reinforced Cu10Sn material.

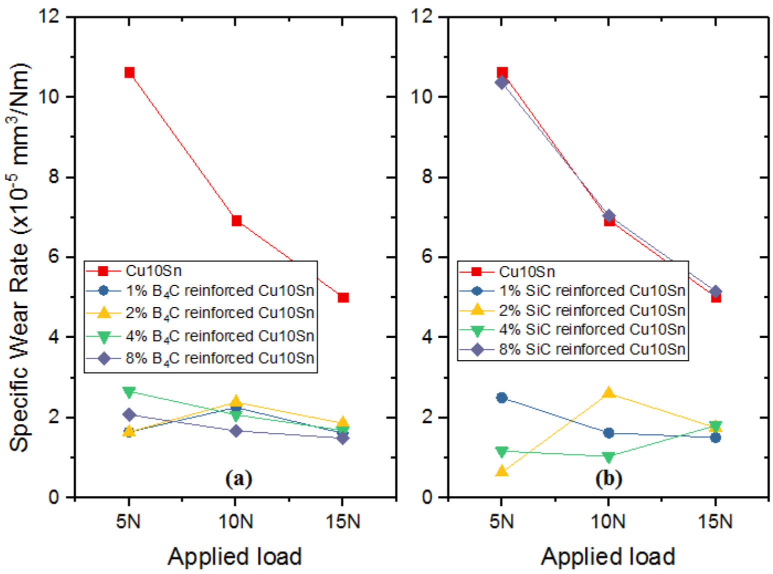


**Fig. 9.** Wear coefficient graph of $B_4C$ (a) and SiC (b) reinforced Cu10Sn material.

The friction coefficient (CoF) values obtained during the wear tests are given in Fig. 10. The average CoF value of the Cu10Sn material was determined to be 0.14 in the test conditions. It has been determined that $B_4C$ and SiC reinforcements do not increase the friction coefficient of Cu10Sn material, and even slightly reduce it in some reinforcement materials and reinforcement ratios. In addition, a smooth friction coefficient graph was obtained during the wear test except for the 8% $B_4C$, and SiC-reinforced Cu10Sn test samples. The frictional fluctuation between the pin-disc as a result of the rupture of the reinforcement materials emerging to the surface with wear, that is, the increase of the abrasive effect of the ruptured reinforcement elements, may cause this situation. It is thought that this situation occurs as a result of the increase in fragility, especially with the increase of the amount of carbon, above certain reinforcement ratios in the 8% reinforced samples. In the study, despite the increase in hardness in Alloy 5 and Alloy 9, where an 8% reinforcement rate was applied, it was found that the wear resistance decreased. Depending on the type of reinforcement, this may occur after the addition of certain amounts of reinforcement material [46, 47].

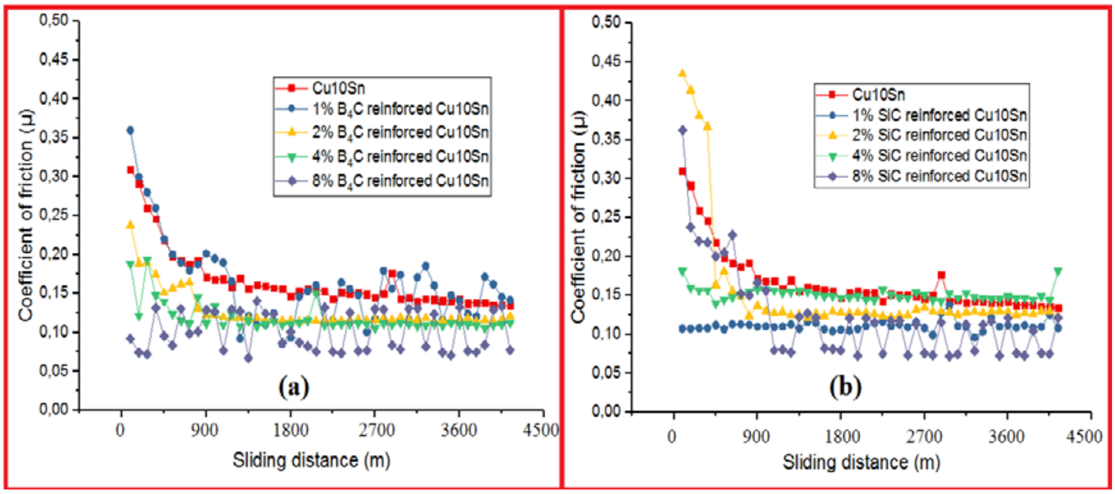


**Fig. 10.** Coefficient of friction (a) $B_4C$ reinforced Cu10Sn (b) SiC reinforced Cu10Sn.

Abraded surface FESEM images of 2% $B_4C$, 8% $B_4C$ and 2% SiC, and 8% SiC composite structures added to Cu10Sn alloy under 15N load are given in Fig. 11. After the wear tests, it is seen that there are traces, cavities, and debris on the material's surface. The Cu-Sn alloys produced by the P/M method are similar to the possibly corroded surface images [48]. Worn surface images of Cu10Sn material without reinforcement in (a) and (b), 2% and 4% $B_4C$ reinforced in (c) and (e), and 2% and 4% SiC reinforced in (d) and (f) have been given, respectively.

Oxidation-induced whiteness is observed on the surface of the unreinforced material and 2% $B_4C$ reinforced material. During friction, the surface of the pin (Cu10Sn) and disc (AISI 52100) is welded to each other due to pressure and temperature, resulting in breaks (adhesive wear). As a result of these adhesions, oxidation occurs on the surfaces that break. It was determined that the highest volume loss in Cu10Sn composite reinforced in different proportions occurred in the sample supplemented with 8% SiC. Worn surface images also prove this situation. The surface of the 8% SiC reinforced Cu10Sn material, which has a worn surface appearance in Fig. 11 (f), is damaged due to breaks, adhesions, and debris.

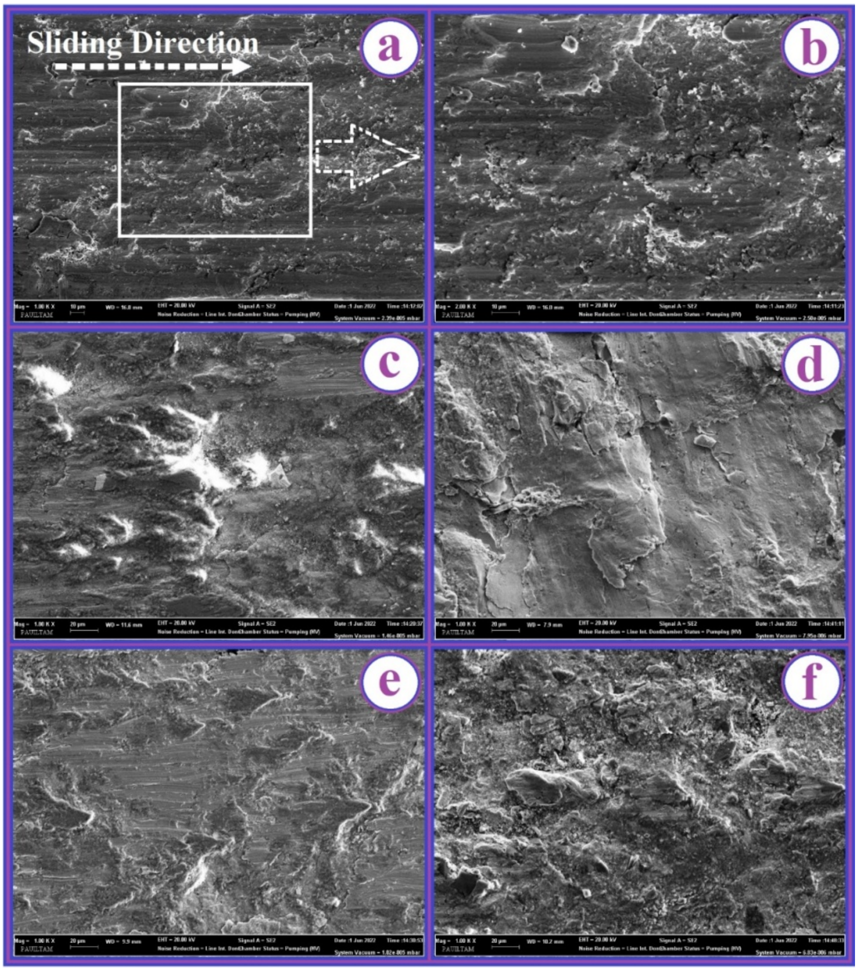


**Fig. 11.** FESEM Images; a, b) Different magnifications of Cu10Sn alloy (X1000, X2000).

When Fig. 12 is examined, there are EDS peaks and element distribution ratios taken from FESEM images and FESEM images after wear under 15N load of 2% $B_4C$, 8% $B_4C$, and 2% SiC, 8% SiC composite structures added to Cu10Sn alloy. Fig. 12 (a) shows the corroded surface FESEM image of the main alloy content (Cu10Sn) and (a1) shows the element intensities and element distribution ratios taken from the FESEM image (it is the region within the yellow area). When the elements in Fig. 12 a.1 are examined as wt.%, it is seen that Cu from the main alloy in the structure has 77.05, Sn 6.64, C 8.35, and O 7.27 content ratios. Cu and Sn contents are the main additives in the structure, and O and C are known as residues of C contents formed by an oxide layer with open surface formation after wear [49, 50], and taken from the structure after contact with the abrasive disc. These layers formed on the surface positively affect the wear behavior thanks to their lubrication duties [51]. In this study, these layers, which are naturally obtained in wear processes, can also be added to assume the role of lubrication [52-55]. In Fig. 12, (b), (b.1) and (c), (c.1), respectively, the EDS peak and element distributions taken from the FESEM images of Cu10Sn +2% $B_4C$ and Cu10Sn +8% $B_4C$ composite structures are given. When the analyses taken from the images of Fig. 12, (b), (b.1) and (c), (c.1) are examined, there are B and C contents formed by the addition of $B_4C$ next to Cu and Sn from the main additions in the structure. It is also seen that there is Fe and C content originating from the abrasive disc. It has been observed that O content is encountered due to the oxide layer formed after wear test. In Fig. 12, (d), (d.1) and (e), (e.1), respectively; EDS peak and element distributions taken from FESEM images and

FESEM images of Cu10Sn +2% SiC and Cu10Sn +8% SiC composite structures are included. When the analyzes taken from the images of Fig. 12, (d), (d.1) and (e), (e.1) are examined, it can be seen that the structure contains the Si and C contents formed by the addition of SiC in addition to the Cu and Sn from the main additions. It is also seen that there is Fe and C content originating from the abrasive disc. It was also seen in the analysis that O content was encountered due to the oxide layer formed after wear tests.

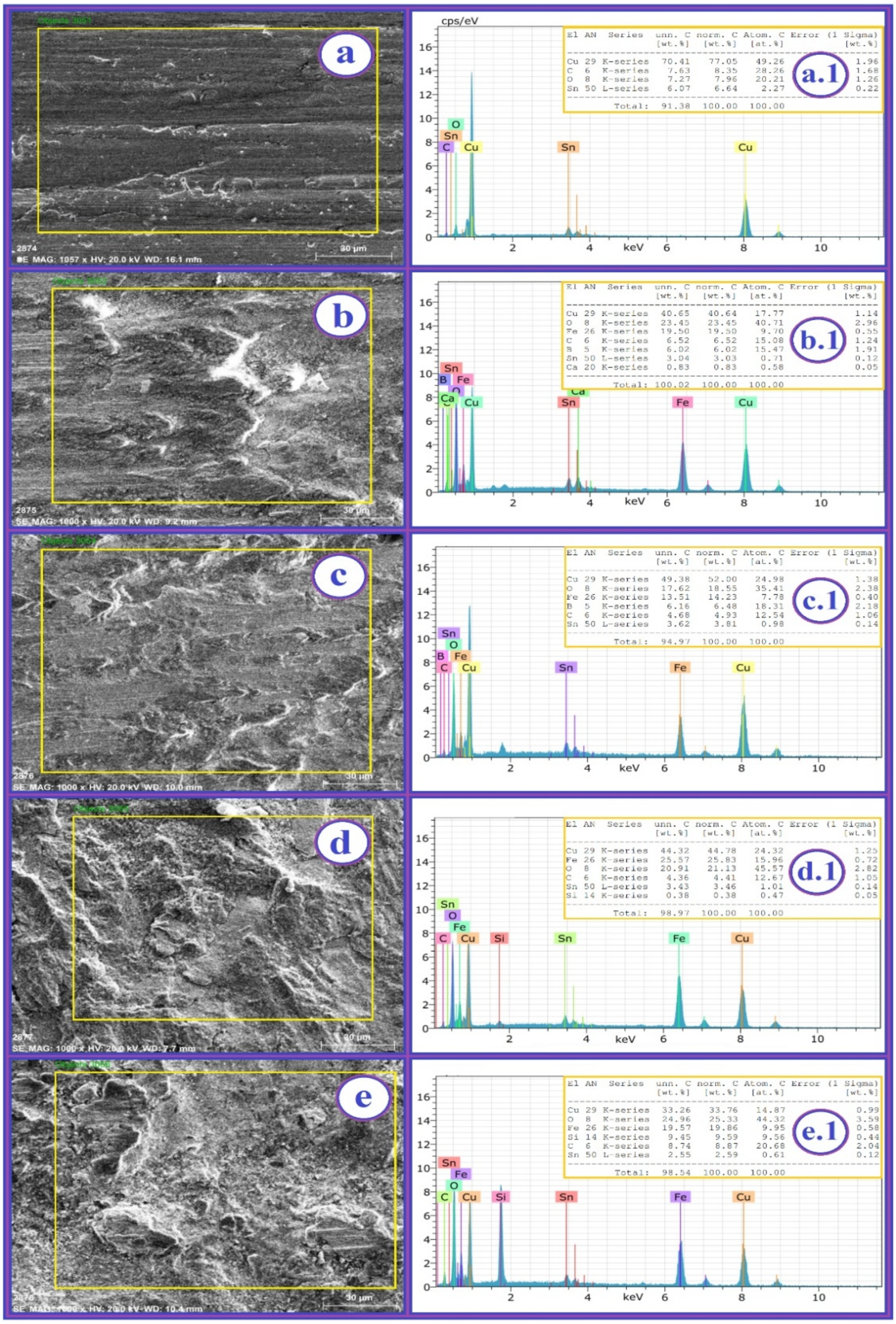


**Fig. 12.** EDS data obtained from FESEM images and images.

When the general evaluation is made after wear experiments, it is known that an increase in the hardness of the structure occurs thanks to the composite reinforcements added to Cu10Sn alloys [48], and it has been observed that the increased reinforcement rates positively affect the volume losses [56]. It has also been observed that the mechanical and wear behavior of the composite contents added to Cu-Sn alloys can be improved in the material [57].

When the microhardness and wear graphs were evaluated together; in microhardness graphs, it was determined that the highest results were obtained in $B_4C$ and SiC reinforced composite materials with 4% and 8% reinforcement. In the wear graphs, the best results were obtained with the lowest volume loss, specific wear rate and average coefficient of friction values in 8% $B_4C$ reinforced material, while the best results were obtained in SiC reinforced materials at 4% reinforcement ratio. When both reinforcement materials were evaluated together for the microhardness and wear tests, it was seen that optimum results were achieved for $B_4C$ in 8% and 4% reinforced composite materials, and for SiC in 4% reinforced composite material.

## 4. Conclusion

It was understood from the microstructure and SEM images that $B_4C$ and SiC particles showed a homogeneous distribution in the bronze matrix structure.

- In general, the microhardness values of the samples increased with the addition of $B_4C$ and SiC. In the results; due to the fact that there are carbide-based particles that increase hardness in composite materials, a direct proportional increase in hardness is noteworthy with the increase in $B_4C$ and SiC reinforcement ratios.
- The volume loss and SWR values of Cu10Sn material added at different rates of $B_4C$ were measured lower than those of unreinforced Cu10Sn at all additive rates. In general, the same was true except for the SiC reinforced test samples.
- When the reinforcement ratios were compared, it was determined that there was no significant difference between the volume loss values. As a result of the wear tests, the lowest volume loss rates were measured in 8% $B_4C$ and 4% SiC reinforced composite materials. With the increase in the applied load, an increase in volume loss occurred in all the test parameters, as expected.
- The average coefficient of friction (CoF) value obtained during the wear experiments was determined as approximately 0.14. It has been determined that $B_4C$ and SiC reinforcements do not increase the friction coefficient of Cu10Sn material, and even slightly reduce it in some reinforcement materials and reinforcement ratios.
- When the FESEM images of the worn surface of the $B_4C$ and SiC composite structures added to the Cu10Sn alloy are examined under 15N load, it is found that there are traces, voids and debris on the material surface; and that in some areas, it was observed that whiteness developed due to oxidation.
- During friction, the surface of the pin (Cu10Sn) and the disc (AISI 52100) have been combined to each other with the effect of pressure and temperature, and have been subjected to breakage. As a result of these adhesions, oxidation occurred on the broken surfaces.
- When the microhardness and the wear results were evaluated together, it was seen that optimum results were obtained in 4% - %8 $B_4C$ and 4% SiC reinforced alloys (Alloy4 - Alloy5 and Alloy8).

## Acknowledgments

This study was supported by TUBITAK 2209-A National Undergraduate Students Research Projects Support Program. The authors would like to thank The Scientific and Technological Research Council of Türkiye (TUBITAK). The authors would also like to thank Kastamonu University and Pamukkale University for providing research facilities.

## 5. References

1. İ. Uygur, Iranian J. Science & Techn., 28 (2004) 239-248.
2. A.T. Saleem et al., Science of Sintering, 53 (2021) 127-136.
3. Y. Kaplan, S. Aksöz, H. Ada, E. İnce, S. Özsoy Science of Sintering, 52(4) (2020) 445-456.
4. S. Aktaş and E. A. Diler, Int. Adv. Res. and Eng. J. 02(01) (2018) 68-74.
5. M. Uzun, M. M. Munis, Ü.A. Usca. J. Eng. Res. Appl. 8(7) (2018) 1-7.
6. Ü.A. Usca, M. Uzun, M. Kuntoğlu, S. Şap, K. Giasin, D. Y. Pimenov, Materials. 14(15) (2021) 4217.
7. S. Şap, M. Uzun, Ü. A. Usca, D. Y. Pimenov, K. Giasin, S. Wojciechowski, J. Mater. Res. Technology, 15 (2021) 6990-7003.
8. E. Sap, J. Mater. Eng. Perform. 29 (2020) 8461-8472.
9. M. Uzun, M. S. Çetin. Adv. Powder Technology 32(6) (2021) 1992-2003.
10. M. Akbarpour, E. Salahi, F. A. Hesari, E.Y. Yoon, H. S. Kim, A. Simchi, Mater Sci Eng A., 568 (2013) 33-39.
11. M. Uzun, M. M. Münis, Ü. A. Usca, Sakarya Unıversıty Journal of Scıence, 22(2) (2018) 495-501.
12. A. Jamwal, P. P. Seth, D. Kumar, R. Agrawal, K. K. Sadasivuni, P. Gupta, Mater. Chem. and Phys. 251 (2020) 123090.
13. U. A. Usca, M. Uzun, S. Şap, M. Kuntoğlu, K. Giasin, D. Y. Pimenov, S. Wojciechowski, J. Mater. Res. and Techn., 16 (2022) 1243-1259.
14. R. Nithesh, N. Radhika, S. S. Sunder, J. Tribol. 139 (2017) 061603.
15. P.K. Prajapati, D. Chaira, Trans. Indian Inst. Met. 72 (2019) 673-684.
16. S. F. Moustafa, Z. Abdel-Hamid, A. M. Abd-Elhay, Mater Lett, 53 (2002) 244.
17. B.S. Ünlü, N.S. Köksal, E. Atik, C. Meriç, Pamukkale University Journal of Engineering Sciences, 11,1 (2005) 41-45.
18. A. B. Backensto, in: "Advances in Powder Metallurgy", Ed. P. J. McGeehan, Metal Powder Industry Publishing, Pittsburgh, 1990, p. 303-314.
19. G. C. Pratt, International Metallurgical Reviews, 18:2 (1973) 62-88.
20. M. Chmielewski, S. Nosewicz, E. Wyszkowska, Ł. Kurpaska, A. Strojny-Nędza, A. Piątkowska, et al., Ceram Int. 45(7) (2019) 9164-9173.
21. M. Uzun, Ü.A. Usca, Dicle University Journal of Engineering, 8(4) (2017) 797-803.
22. M. Barmouz, P. Asadi, M. K. B. Givi, M. Taherishargh, Mater Sci Eng A. 528, 3 (2011) 1740-1749.
23. E. Çelik, A. K. Aslan, Science of Sintering, 49, 3 (2017) 225-234.
24. G. Cui, J. Ren, Z. Lu, Tribology Letter, 65, 3 (2017) 108.
25. S. Islak, U. Çalıgülü, H.R.H. Hraam, C. Özorak, V. Koç, Res. Eng. Struct. Mater., 5, 2 (2019) 137-146.
26. P. H. Nayak, M. R. Prakash, V. Vinay, et al. International Journal of Metalcasting, 17 (2023) 1266-1276.
27. H. Torabi, R. Arghavanian, J. Alloys Compd., 806 (2019) 99-105.
28. A. M. Hassan, A. Alrashdan, M. T. Hayajneh, A. T. Mayyas, Tribology International, 42, 8 (2009) 1230-1238.

29. A. Mazahery, M. O. Shabani, Composites Part B: Engineering, 43:3 (2012) 1302-1308.
30. S. Islak, A. M. Abushraida, Sakarya University Journal of Science, 23(6) (2019) 1137-1143.
31. H. İpek, European Journal of Engineering and Natural Sciences, 2(1) (2017) 102-107.
32. G. Veerappan, D. Pritima, S. Marichamy, V. Dhinakaran, S. Sathish, Materials Today: Proceedings, 74 (2022) 44-48.
33. B. Bunlangsup, C. Auechalitanukul, R. McCuiston, Materials Today: Proceedings, 5(3) (2018) 9250-9255.
34. M. S. Shunmugam, P.K. Philip, A. Gangadhar, Tribology International, 26(2) (1993) 109-113.
35. R. Abhik, V. Umasankar, M. A. Xavior, Procedia Eng., 97 (2014) 941-950.
36. Y. Xing, N.Y. Li, C.J. Li, P. Gao, H.D. Guan, C.M.Y. Yang, C.J. Pu, J.H. Yi, Materials Science and Engineering: A, 851 (2022) 143664.
37. J. Wu, Z. Li, Y. Luo, Z. Gao, Y. Li, Y. Zhao, Ya. Liao, C. Wu, M. Jin, Ceramics International, 49(2) (2023) 2978-2990.
38. T. Yener, et al., Acta Physica Polonica A, 127:4 (2015) 1045-1047.
39. G. Celebi Efe, S. Zeytin, C. Bindal, Materials & Design (1980-2015), 36 (2012) 633-639.
40. E. Asikuzun, A. Donmez, L. Arda, O. Cakiroglu, O. Ozturk, D. Akcan, M. Tosun, S. Ataoglu, C. Terzioglu, Ceramics International, 41(5) (2015) 6326-6334.
41. S. Celik, O. Ozturk, E. Coskun, M. Sarıhan, E. Asikuzun, K. Ozturk, C. Terzioglu, J. Mater. Sci: Mater. Electron., 24 (2013) 2218-2227.
42. A. Mavi, Y. Kaplan, S. Aksoz, Journal of Tribology, 143(12) (2021) 121702.
43. E. Sap, Ceramics International, 47, 18 (2021) 25910-25920.
44. P. Lakshmanan, S. Dharmaselvan, S.Paramasivam, L. K. Kirubanandan, Vignesh R, Materials Today: Proceedings, 16, 2 (2019) 584-591.
45. G. E. Kiourtsidis, S. M Skolianos, Wear, 253: 9–10 (2002) 946-956.
46. N. Y. Çolak, H. Turhan, Science and Eng. J. of Fırat Univ., 28 (2) (2016) 259-266.
47. İ. Topcu, A. N. Güllüoğlu, M. K. Bilici, H. Ö. Gülsoy, J. Fac. of Eng. and Arch. of Gazi Univ. 34(3) (2018) 1441-1450.
48. H. M. Mallikarjuna, K. T. Kashyap, P. G. Koppad, C. S. Ramesh, R. Keshavamurthy, Transactions of Nonferrous Metals Society of China, 26(7) (2016) 1755-1764.
49. J. F. Li, L. Zhang, J. Xiao, K. Zhou, Transactions of Nonferrous Metals Society of China, 25(10) (2015) 3354-3362.
50. K. Kang, G. Bae, B. Kim, C. Lee, Surface and Coatings Technology, 206(19-20) (2012) 4060-4067.
51. Ö. Pamuk, Y. Kaplan, S. Aksöz, Powder Metallurgy and Metal Ceramics, 60 (2021) 439-450.
52. D. Sımsek, D. Ozyurek, Journal of Tribology, 142(10) (2020) 101701.
53. G. Rajaram, S. Kumaran, T. S. Rao, M. Kamaraj, Tribology International, 43(11) (2010) 2152-2158.
54. D. Şimşek, D. Özyürek, S. Salman, Industrial Lubrication and Tribology, 74(5) 2022 463-471.
55. G. Rajaram, S. Kumaran, T. S. Rao, Tribology Transactions, 54 (2011) 115-121.
56. P. S. Kumar, K. Manisekar, E. Subramanian, R. Narayanasamy, Tribology Transactions, 56 (2013) 857-866.
57. K. E. Öksüz, Advanced Materials Research, 1128, (2015) 123-126.


***Сажетак:*** *Да би се постигла боља механичка својства легуре бронзе, важно је производити нове материјале додавањем ојачања и понудити ове материјале*

*индустрији. У овој студији, материјали бронзане матрице (Cu10Sn) су ојачани керамичким материјалима од бор карбида ($B_4C$) и силицијум карбида (SiC) методом механичког легирања. Нови композитни материјали произведени су методом металургије праха додавањем керамичке арматуре ($B_4C$ и SiC) у тежинским односима 1, 2, 4 и 8 у легуру Cu10Sn, која је главни материјал матрице. Добијени композитни материјали су испитани у погледу структурне, микротврдоће и отпорности на хабање. За произведене узорке испитивани су коефицијент трења, специфична стопа хабања и стопе губитка запремине под оптерећењем од 5N, 10N и 15N. Када су испитани примењена микротврдоћа и понашање при хабању, генерално се видело да су тврдоћа и понашање хабања побољшани са додатним односима ојачања. У складу са извршеним испитивањима, на основу процеса тврдоће и хабања примењених на материјале који се састоје од бронзане матрице арматурног материјала, уочено је да су најприкладнији резултати добијени од композитних материјала (Легура 4 и Легура 8), који садрже 4% $B_4C$ и SiC ојачања.*
***Кључне речи**: Металургија праха, бронза, композит, хабање, микротврдоћа.*